ESC European Society of Cardiology

Cardiovascular Research (2018) **114**, 1525–1535
doi:10.1093/cvr/cvy111

DNA methylation of a *PLPP3* MIR transposon-based enhancer promotes an osteogenic programme in calcific aortic valve disease

Ghada Mkannez[1], Valérie Gagné-Ouellet[2,3], Mohamed Jalloul Nsaibia[1], Marie-Chloé Boulanger[1], Mickael Rosa[1], Deborah Argaud[1], Fayez Hadji[1], Nathalie Gaudreault[4], Gabrielle Rhéaume[1], Luigi Bouchard[2,3], Yohan Bossé[4], and Patrick Mathieu[1]*

[1]Laboratory of Cardiovascular Pathobiology, Department of Surgery, Quebec Heart and Lung Institute/Research Center, Laval University, QC, Canada; [2]Department of Biochemistry, Université de Sherbrooke, Sherbrooke, QC, Canada; [3]ECOGENE-21 Biocluster, Chicoutimi Hospital, Saguenay, QC, Canada; and [4]Department of Molecular Medicine, Laval University, QC, Canada

Received 13 November 2017; revised 27 February 2018; editorial decision 24 April 2018; accepted 1 May 2018; online publish-ahead-of-print 2 May 2018

Time for primary review: 36 days

Aims Calcific aortic valve disease (CAVD) is characterized by the osteogenic transition of valve interstitial cells (VICs). In CAVD, lysophosphatidic acid (LysoPA), a lipid mediator with potent osteogenic activity, is produced in the aortic valve (AV) and is degraded by membrane-associated phospholipid phosphatases (PLPPs). We thus hypothesized that a dysregulation of PLPPs could participate to the osteogenic reprograming of VICs during CAVD.

Methods and results The expression of PLPPs was examined in human control and mineralized AVs and comprehensive analyses were performed to document the gene regulation and impact of PLPPs on the osteogenic transition of VICs. We found that *PLPP3* gene and enzymatic activity were downregulated in mineralized AVs. Multidimensional gene profiling in 21 human AVs showed that expression of *PLPP3* was inversely correlated with the level of 5-methylcytosine (5meC) located in an intronic mammalian interspersed repeat (MIR) element. Bisulphite pyrosequencing in a larger series of 67 AVs confirmed that 5meC in intron 1 was increased by 2.2-fold in CAVD compared with control AVs. In isolated cells, epigenome editing with clustered regularly interspersed short palindromic repeats-Cas9 system containing a deficient Cas9 fused with DNA methyltransferase (dCas9-DNMT) was used to increase 5meC in the intronic enhancer and showed that it reduced significantly the expression of *PLPP3*. Knockdown experiments showed that lower expression of PLPP3 in VICs promotes an osteogenic programme.

Conclusions DNA methylation of a MIR-based enhancer downregulates the expression of PLPP3 and promotes the mineralization of the AV.

Keywords Calcific aortic valve disease • Aortic stenosis • Epigenetics • PLPP3 • PPAP2B • Valve interstitial cells • Lipid phosphate phosphatase • Phospholipid phosphatase • Enhancer • DNA methylation • H3K27me3 • BMP2 • RUNX2

1. Introduction

Calcific aortic valve disease (CAVD) is a prevalent heart valve disorder, which is characterized by the mineralization of the aortic valve (AV). During CAVD, valve interstitial cells (VICs), which have a high plasticity, undergo an osteogenic reprograming.[1] So far, the process whereby VICs undergo a phenotypic switch towards osteogenic reprograming remains largely elusive. The epigenome is regarded as an important regulatory

* Corresponding author: Institut de Cardiologie et de Pneumologie de Québec/Québec Heart and Lung Institute, 2725 Chemin Ste-Foy, QC G1V-4G5, Canada. Tel: +1 418 656 8711; fax: +1 418 656 4707, E-mail: patrick.mathieu@fmed.ulaval.ca

layer that allows cell reprograming.[2] Previous work highlighted that altered DNA methylation during CAVS may participate to gene reprograming.[3] Methylation of CpG sites as well as histone modifications exert a crucial control over the expression of genes by modifying the accessibility of DNA to the transcription factors and cofactors. In this regard, enhancers, which are regulatory elements that interact with promoters, are regulated through epigenetic processes.[4] Enhancers may reside in large intergenic regions or may be located within introns. A large portion of the genome consists in transposable elements (TEs), which have been exapted throughout evolution as regulatory loci of the genome.[5] For instance, mammalian interspersed repeat (MIR) elements are enriched in regions containing enhancers, which have low level of 5-methylcytosine (5meC) when active.[6] In this regard, cytosine methylation of enhancers has been proposed to act as a memory during developmental processes to ensure tissue-specific gene expression pattern.[7] During the development of complex trait disorders, such as CAVD, the gene expression pattern is considerably modified.[8,9] Whether cytosine methylation-dependent memory of key enhancers is altered in CAVD is presently unknown.

Mendelian randomization studies have underlined that low-density lipoprotein cholesterol (LDL) and lipoprotein(a) [Lp(a)] are causally related to CAVD.[10,11] Lp(a) is major carrier of oxidized phospholipids (OxPLs).[12] In mice, the progression of CAVD is largely dependent on the production of lysophosphatidic acid (LysoPA), a small bioactive lipid derivative presents in human mineralized AVs and generated from OxPLs by autotaxin (ATX).[13] ATX is a lysophospholipase D enzyme enriched in the Lp(a) fraction and secreted by VICs.[13,14] Oxidized LDL (OxLDL) promotes the osteogenic reprograming of VICs through a LysoPA receptor 1-dependent pathway, which activates *BMP2*, a potent promoter of osteogenic transdifferentiation.[15] Membrane-associated enzymes of the phospholipid phosphatases (PLPPs) family degrade bioactive lipid derivatives including LysoPA and may therefore modulate the osteogenic response of VICs.[16] Whether PLPPs are expressed and dysregulated during CAVD is presently unknown. In this work, we identified a novel process whereby cytosine methylation of a MIR retrotransposon-based enhancer promotes a downregulation of phospholipid phosphatase 3 (*PLPP3*/*PPAP2B*) as well as an osteogenic programme during CAVD.

2. Methods

Expanded methods are in the Supplementary material online.

2.1 Procurement of tissues for analyses

We examined stenotic AVs (CAVS) that were explanted from patients at the time of AV replacement. Control non-calcified AVs with normal echocardiographic analyses were obtained during heart transplant procedures. The protocol was approved by the local ethical committee and informed consents were obtained from the subjects. The study conforms with the declaration of Helsinki.

2.2 Real-time polymerase chain reaction

RNA was extracted from valves explanted from patients or from cells during *in vitro* experiments. Total RNA was isolated with RNeasy micro kit from Qiagen (ON, Canada). The RNA extraction protocol was performed according to manufacturer's instructions. The quality of total RNA was monitored by capillary electrophoresis (Experion, Biorad, ON, Canada). One μg of RNA was reverse transcribed using the Qscript cDNA supermix from Quanta (VWR, Canada). Quantitative real-time PCR (qPCR) was performed with perfecta sybr supermix from Quanta on the Rotor-Gene 6000 system (Corbett Robotics Inc, CA, USA). Primers for *PLPP3* (cat no. QT00052836), *RUNX2* (cat no. QT00020517), *BGLAP* (cat no. QT00232771), and *BMP2* (cat no. QT00012544) were obtained from QIAGEN (ON, Canada). The expression of the hypoxanthine-guanine phosphoribosyltransferase (*HPRT*, cat no. QT00059066) gene (QIAGEN, ON, Canada) was used as a reference to normalize the results.

2.3 Western blotting

Tissue pieces were mixed with lysis buffer (150 mM NaCl, 20 mM Tris pH7.5, 10% glycerol, 5 mM EGTA, 0.5 mM EDTA, 2 mM sodium vanadate, 50 mM sodium fluoride, 1% triton X-100, 0.1% Sodium dodecyl sulphate (SDS), 80 mM β-glycerophosphate, 5 mM sodium pyrophosphate, 1 mM PMSF and protease inhibitor cocktail). Mechanical lysis was performed by using a polytron, followed by centrifugation at 300 *g* for 10 min at 4°C, supernatants were harvested and protein loading buffer was added. Cells were harvested in protein loading buffer. Samples were boiled 5 min, proteins were loaded onto polyacrylamide gels followed by electrophoresis and transferred onto nitrocellulose membranes. Membranes were blocked with TBS-tween containing 5% non-fat dry milk and incubated with either PLPP3 (Novus Biologicals, ON, Canada) or β-ACTIN (Sigma-Aldrich, ON, Canada) primary antibodies overnight at 4°C. Membranes were then washed and incubated with HRP-labeled secondary antibodies (Cell Signaling Technology, MA, USA). Detection was done using clarity western ECL substrate (BioRad, ON, Canada). Images were acquired and quantification analyses were performed using a ChemiDocMP system (BioRad, ON, Canada).

2.4 Measurement of phosphate lipid phosphatase phosphohydrolase activity in tissue homogenates

Control non-mineralized and CAVD valve tissues were homogenized and harvested in lysis buffer 20 mM Tris HCl, pH7.5, 1 mM EGTA, 1 mM, 1 mM DTT, 1× PIC (protease inhibitor cocktail, SIGMA, ON, Canada). Homogenates were centrifuged at 500 g for 5 min and supernatant were used for protein assay. The reaction was allowed to proceed with 1ug of protein at 37°C for 30 min in 200 μl of reaction buffer consisting of 20 mM Tris HCl, pH7.5, 1 mM $MgCl_2$, 1 mM DTT and 100 μM LPA. Malachite Green Phosphate Detection Kit was used to measure the phosphatase activity of PLPP3, according to the manufacturer's instructions.

2.5 Quantification of LysoPA by conventional thin-layer chromatography

CAVD valve tissues (10 mg for every specimen) were homogenized for 30 s in chloroform-methanol (2:1), 1% butylated hydroxytoluene (BHT), incubated 2 h at room temperature and centrifuged 5 min at 800 *g* at 4°C. Samples were then extracted in chloroform:methanol (1:1), 0.5% BHT, incubated at room temperature 2 h and centrifuged. The last extraction step was performed in chloroform:methanol (1:2), 0.5% BHT, incubated 2 hurs at room temperature and centrifuged. The chloroform phases were pooled and samples were evaporated to dryness. Extracts were dissolved in 100 μl chloroform:methanol (3:2), 0.5% BHT. A 20 μl was applied to a thin-layer chromatography plate (20 × 20 cm) and 20 μg of LPA standard was applied. Visualization was performed using 0.1%

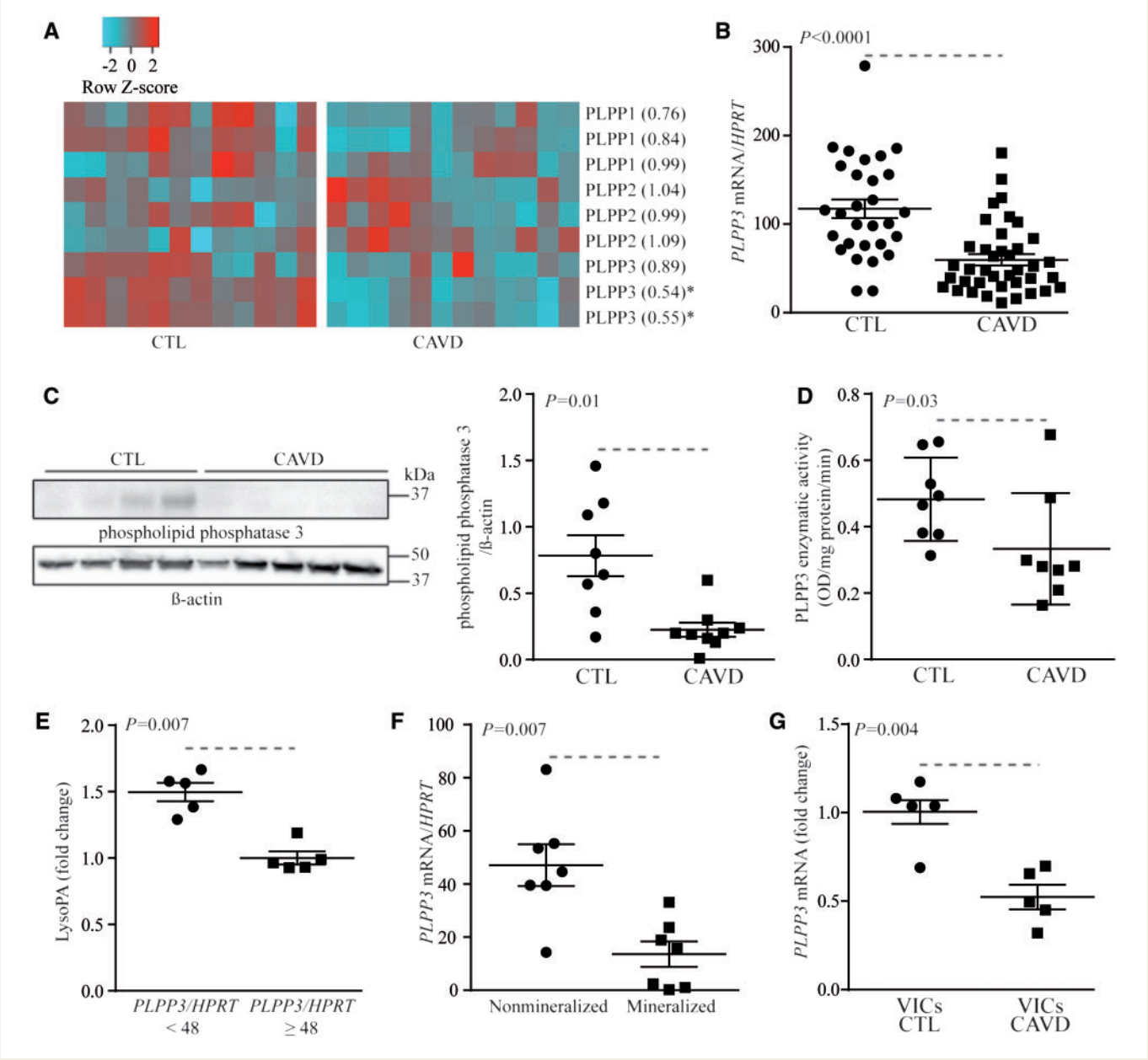

Figure 1 Expression of PLPP3 is reduced in CAVD. (*A*) Transcriptome of *PLPP*s in CTL ($n = 12$) and CAVD specimens ($n = 12$), the number in parentheses following the gene name represents the relative change in expression (*indicates $P < 0.05$). (*B*) mRNA levels for *PLPP3* in CTL ($n = 29$) and CAVD ($n = 39$) ($P < 0.0001$). (*C*) Western blotting for PLPP3 showing a representative experiment and the quantification in CTL ($n = 8$) and CAVD ($n = 9$) ($P = 0.01$). (*D*) PLPP enzyme activity in CTL (n = 8) and CAVD ($n = 8$) ($P = 0.03$). (*E*) LysoPA relative levels according to *PLPP3* mRNA levels (divided at median) ($n = 10$) ($P = 0.007$). (*F*) *PLPP3* mRNA levels in pathologic aortic valves (CAVD) according to the state of mineralization ($n = 7$) ($P = 0.007$). G) *PLPP3* mRNA levels in VICs isolated from CTL ($n = 5$) and CAVD ($n = 5$) ($P = 0.004$). Values are mean ± SEM, (*B*) Student *t*-test, (*C–G*) Wilcoxon-Mann-Whitney statistical analyses; CTL, control; CAVD, calcific aortic valve disease.

Amido Black 10 b in 1 M NaCl and tissues compared on relative scale by using band intensity by using iCY platform (http://icy.bioimageanalysis.org/).

2.6 Whole-genome gene expression and DNA methylation

Total RNA was extracted from 100 mg of tissue using the RNeasy Plus Universal Mini Kit (QIAGEN, ON, Canada) according to manufacturer's protocol. Concentration was evaluated by UV measurement using the Nanovue spectrophotometer (GE Healthcare LifeScience, NJ, USA). RNA quality was assessed using the Agilent 2100 Bioanalyzer (Agilent Technologie, CA, USA). Expression was measured on the HumanHT-12 v4 Expression BeadChip from Illumina (CA, USA). Samples were removed based on outliers in pairwise correlation, principal components analysis and hierarchical clustering. Probes were excluded of the current analysis if the detection call rate was >0.2 (if the probes was detected in at least five patients). mRNA expression data were log2 transformed and quantile normalized prior to analysis, using R 3.0.0 statistical software and the Bioconductor package lumi. Methylation sites were

Table I Clinical characteristics of patients for qPCR analyses

	Control valves ($n = 29$)	CAVD ($n = 39$)	*P*-value
Age	49 ± 3	69 ± 2	<0.0001
Male (%)	76	51	0.14
Smoking (%)	3	8	0.4
Hypertention (%)	34	76	0.001
Diabetes (%)	21	31	0.41
Coronary heart disease (%)	34	38	0.8
Bicuspid AVs (%)	0	51	<0.0001
BMI (kg/m^2)	28.8 ± 1.1	28.6 ± 0.9	0.73
Waist circumference (cm^2)	97.2 ± 5.7	101.0 ± 2.5	0.59
Statins (%)	62	100	<0.001
AV area (cm^2)	–	0.77 ± 0, 04	–
Aortic peak gradient (mmHg)	–	74.2 ± 5.4	–
Aortic mean gradient (mmHg)	–	45.6 ± 3.5	–
Triglycerides (mmol/l)	1.80 ± 0.26	1.75 ± 0, 18	0.9
LDL (mmol/l)	2.13 ± 0.22	2.29 ± 0, 14	0.49
HDL (mmol/l)	1.04 ± 0.08	1.31 ± 0.072	0.04
Creatinine (μmol/l)	111.5 ± 7.3	87.6 ± 3.6	0.006
Creatinine clearance (ml/min)	77.1 ± 7.2	67.1 ± 3.8	0.27

Values are mean ± S.E.M. or %; BMI, body mass index; LDL, low-density lipoprotein; HDL, high-density lipoprotein.

interrogated on the Illumina Infinium HumanMethylation450 BeadChip testing 485, 513 CpG sites located in gene promoter, 5'UTR, first exon, gene body and 3'UTR regions, densely methylated regions and methylation islands.

2.7 Pyrosequencing

DNA was purified from AV samples using the QIAamp DNA mini kit (Qiagen).

Briefly, 200 ng of gDNA was treated with sodium bisulphite (EpiTech Bisulfite Kit, Qiagen) and amplified using Pyromark PCR kit (Qiagen). Amplicons were then pyrosequenced on the PyroMark Q24 (Qiagen). Primers were designed with PyroMark Assay Design v2.0.1.15 (Qiagen) (PLPP3-forward: 5'-AAGGGGTTTTGGAGAGTAT-3', PLPP3-reverse: 5'-AAACTTCCAAAATTAAAATCAACCT -3', PLPP3-sequencing: GTTTTGATGATAAGTATTGTG). The assay was designed to measure DNA methylation levels of cg02468627. cg02468627 co-localizes with rs111513408 (A/G) (MAF A = 1.1%); rare subjects with the minor allele A were excluded from the study.

2.8 Chromatin immunoprecipitation

Tissues were homogenized in 1 ml of phosphate-buffered saline (PBS)1× containing PIC (Sigma, ON, Canada). The homogenized samples were centrifuged 5 minutes at 800 g at 4°C. The supernatants were removed and pellets were resuspended in PBS1× containing PIC and centrifuged 5 min at 800 g at 4°C. Pellets were then resuspended in 500 µl lysis buffer (50 mM Hepes-KOH, pH7.5, 140 mM NaCl, 1 mM EDTA pH8.0, 1% triton X-100, 0.1% sodium deoxycholate, 0.1% SDS, PIC) and sonicated to an average length of 400 base pairs. Antibodies against H3K27me3, H3K4me1 and H3K4me3 or isotype IgG (Cell Signaling, MA, USA) were incubated with proteins G dynabeads (Life technologies, Thermofisher, ON, Canada) for 6 h before DNA samples were added to the antibodies/dynabeads mixtures and incubated at 4°C overnight on a rotator. The next day, the samples were washed with low salt buffer (0.1% SDS, 1% triton X100, 2 mM EDTA, 20 mM Tris HCl pH8.0, and 150 mM NaCl), then with high salt buffer (0.1% SDS, 1% triton X100, 2 mM EDTA, 20 mM Tris HCl pH8.0, and 500 mM NaCl), followed with LiCl buffer (10 mM Tris-HCl, pH8.0, 250 mM LiCl, 1 mM EDTA, pH8.0, 1% NP-40) and finally with TE buffer (10 mM Tris-HCl, pH8.1, 1 mM EDTA, pH8.0). The complex was then eluted from dynabeads by adding 200 µl of elution buffer (1% SDS, 100 mM $NaHCO_3$) at 65°C for 1 h. Eluted samples were reverse cross-linked at 65°C overnight. DNA fragments were purified using phenol-chloroform and samples were analysed by quantitative PCR assay using primers specific to the enhancer region: forward 5'-GTCTGTGCAGGAGCTGTATT-3', reverse 5'-AAGAGCGGTGGGAGTTAAAG-3'.

2.9 Cell transfection

HEK293T cells were transfected by using the calcium phosphate technique. VICs were transfected using Nanojuice transfection reagent (EMD Millipore, VWR, QC, Canada). Following transfection of dCas9-DNMT3A constructs; pdCas9-DNMT3A-PuroR, no. 71667 and pdCas9-DNMT3A-PuroR (ANV), no. 71684 (Addegene, MA, USA) cells were selected with 2 µg/ml puromycin for 48 h (Wisent, QC, Canada).

2.10 Luciferase reporter assay

HEK-293T cells were transfected with the pGL4.10 luciferase vector (Promega, WI, USA) containing the PLPP3 minimal promoter sequence (-140:-700) with or without the enhancer region located in PLPP3 first intron (Gene synthesis and subcloning, Bio Basic, ON, Canada) along with a vector encoding for the renilla luciferase (Promega, WI, USA) as a reporter for transfection efficiency as well as with the dCas9-DMNT3 constructs where indicated. At 48-h post-transfection, cells were harvested and luciferase activity was measured using the Dual-Luciferase Reporter Assay System, according to manufacturer instructions (Promega, WI, USA).

2.11 *In vitro* analyses of calcification

Cells were incubated for 7 days with a mineralizing medium containing: DMEM + 5% FBS, 10^{-7} M insulin, 50 µg/ml ascorbic acid and NaH_2PO_4 at 2 mM. Cells were then incubated 24 h in 0.6 N HCl, supernatants was harvested and sent for quantification and cells were harvested in 1%SDS, 0.1 N NaOH for protein quantification.

2.12 Determination of calcium concentrations

Calcium content in cell cultures was determined by the Arsenazo III method (Synermed, Monterey Park, CA, USA), which relies on the specific reaction of Arsenazo III with calcium to produce a blue complex. Results are measured at 650 nm on the Modular P800 Elecsys of Roche Diagnostics apparatus (Roche Diagnostics, QC, Canada). This reaction is specific for calcium. Magnesium is prevented from forming a complex with the reactive. Results were normalized to protein contents for cell culture experiments.

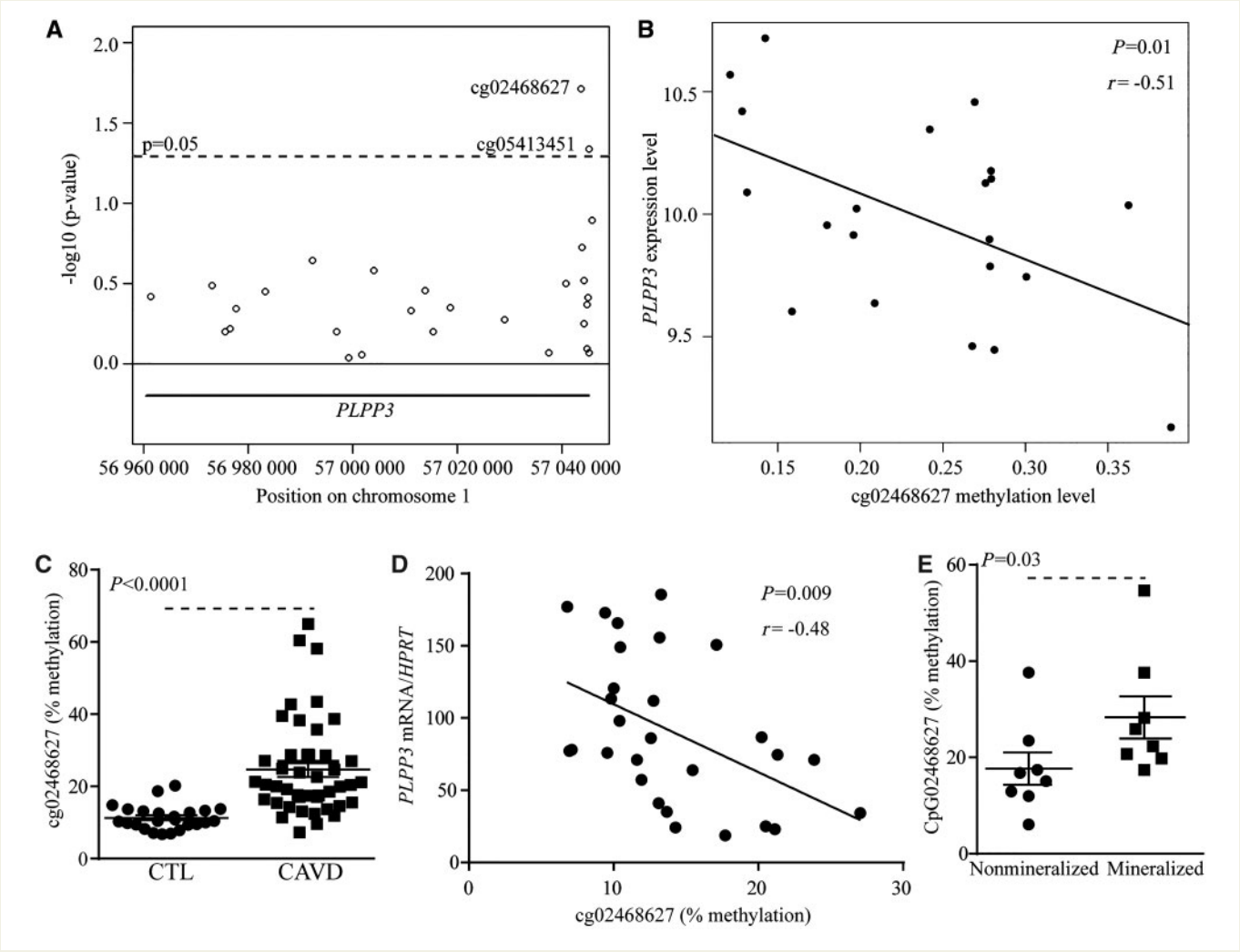

Figure 2 5meC level at cg02468627 inversely correlates with *PLPP3* expression. (*A*) Genomic coordinates (hg19) of CpG sites (open circles) and their relationships with PLPP3 expression represented as –log10 (*P*-value). (*B*) Correlation analysis between the expression of *PLPP3* and CpG methylation level (cg02468627) (n = 21) in CAVD (r = -0.51, P = 0.01). Bisulphite pyrosequencing of cg02468627 in CTL (n = 24) and CAVD (n = 43) (P < 0.0001) (*C*), and correlation analysis between methylation of cg02468627 with *PLPP3* expression (n = 28) (r = -0.48, P = 0.009) (*D*). (*E*) Bisulphite pyrosequencing levels in pathologic aortic valves according to the state of mineralization (n = 8) (P = 0.03). Values are mean ± S.E.M.; (*A*) linear regression model, (*B* and *D*) Pearson's coefficient, (*C*) student *t*-tests, (*E*) Wilcoxon-Mann-Whitney analysis; CTL, control; CAVD, calcific aortic valve disease.

2.13 Determination of alkaline phosphatase activity

VICs were washed with PBS, transferred in 200 µl of 0.2% NP-40, 1 mmol/l $MgCl_2$ and then sonicated. Alkaline phosphatase (ALP) activity was assayed using p-nitrophenyl phosphate as substrate (Sigma, ON, Canada). Samples were incubated in presence of substrate for 30 minutes at 37°C. The ALP activity was then measured by absorbance reading at 410 nm. The assay was carried out in triplicate. Results were normalized to protein content.

2.14 Statistical analyses

Continuous data were expressed as mean ± SEM. Normality of distribution was tested with the Shapiro-Wilk test and data compared with Student *t*-test or Anova when two or more than two groups were compared respectively. For data with a non-normal distribution or a n < 10 data were compared between groups with non-parametric Wilcoxon-Mann-Whitney or Kruskal-Wallis test when two or more than two groups were compared respectively. *Post-hoc* Steel-Dwass multiple comparisons test were performed when the P value of the Kruskal-Wallis test was <0.05. Correlation analyses were performed with Pearson's coefficient. Categorical data were expressed as percentage and compared with Fischer's exact test. For *in vitro* experiments with VICs, n represents the number of experiment performed with different donors. A P-value < 0.05 was considered significant. Statistical analysis was performed with a commercially available software package JMP 13.0 or Prism 6.0.

3. Results

3.1 PLPP3 is downregulated in mineralized AVs

We first examined the expression of *PLPPs* by using whole-genome transcription dataset using array technology and performed in 12 mineralized

Table 2 Clinical characteristics of patients for bisulphite pyrosequencing

	Control valves (n = 24)	CAVD (n = 43)	P-value
Age	50 ± 3	68 ± 1	<0.0001
Male (%)	79	67	0.4
Smoking (%	4	14	0.25
Hypertention (%)	38	72	0.009
Diabetes (%)	13	23	0.35
Coronary heart disease (%)	25	44	0.18
Bicuspid AVs (%)	0	33	<0.0001
BMI (kg/m2)	27.0 ± 1.2	28.9 ± 0.8	0.08
Waist circumference (cm2)	92.5 ± 4.8	104.2 ± 2.2	0.07
Statins (%)	67	97	0.009
AV area (cm2)	–	0.77 ± 0.04	–
Aortic peak gradient (mmHg)	–	66.5 ± 4.3	–
Aortic mean gradient (mmHg)	–	41.4 ± 2.8	–
Triglycerides (mmol/L)	1.42 ± 0.16	1.49 ± 0.12	0.06
LDL (mmol/l)	2.04 ± 0.21	2.10 ± 0.12	0.057
HDL (mmol/l)	1.04 ± 0.07	1.37 ± 0.05	<0.0001
Creatinine (μmol/l)	107.5 ± 7.76	78.0 ± 2.6	0.0007
Creatinine clearance (ml/min)	82.6 ± 8.2	81.1 ± 4.0	0.68

Values are mean ± S.E.M. or %; BMI, body mass index; LDL, low-density lipoprotein; HDL, high-density lipoprotein.

and 12 non-mineralized control AVs (population previously described in[17]). Demographic and clinical data for patients included in the transcriptomic experiment are presented in Supplementary material online, *Table S1*. Among the different PLPPs, *PLPP3/PPAP2B* was reduced significantly in mineralized AVs for two probes testing this gene, whereas the expression levels of other PLPPs were not modified (*Figure 1A*). To support these results, *PLPP3* mRNA levels were measured in an independent series of 39 mineralized and 29 control non-mineralized AVs (*Table 1*). Mineralized and non-mineralized AVs were obtained from AV replacement and heart transplant surgeries respectively. The level of *PLPP3* mRNA was decreased by 49% in mineralized AVs (p< 0.0001; age- and sex-adjusted *P*-value= 0.002) (*Figure 1B*). There is one outlier in the control group, re-analysis without this outlier gave a similar *P*-value (age- and sex-adjusted *P*-value = 0.003). To further corroborate these findings, we next measured the PLPP3 protein level in eight control and nine mineralized AVs. By using western blotting, we documented that the level of PLPP3 was decreased by 71% in mineralized AVs (*Figure 1C*). In the same line, PLPP3 enzymatic activity, which was measured by an assay measuring the release of phosphate from LysoPA, was reduced by 31% in CAVD compared with control non-mineralized AVs (*Figure 1D*). In 10 mineralized AVs, we measured semi-quantitatively the level of LysoPA, a substrate for PLPP3, by using conventional thin-layer chromatography.[13] In the AVs that were used for LysoPA measurement, the level of transcript encoding for *PLPP3* was also measured. Noteworthy, the level of LysoPA was increased by 1.5-fold in AVs with less *PLPP3* mRNA expression (divided at the median) (*Figure 1E*). Next, to address whether the level of mineralization may be associated with *PLPP3* expression we measured the amount of transcripts in macroscopically dissected pathologic AVs into non-mineralized and mineralized areas. In 7 AVs from patients with CAVD, we found that the level of *PLPP3* mRNA was significantly decreased in the mineralized portion compared to non-mineralized area (*Figure 1F*). In isolated VICs, we found that the mRNA level encoding for *PLPP3* was significantly reduced in cells isolated from mineralized AVs when compared with VICs isolated from control non-mineralized valves, even after cell passages (≥3 cell passages) (*Figure 1G*). These data indicate that mineralization of the AV is associated with a downregulation of PLPP3, which could be linked to an epigenetic memory in CAVD.

3.2 Dysregulation of DNA methylation is associated with the level of *PLPP3*

To determine if an epigenetic process could explain the dysregulation of PLPP3 in CAVD, we profiled 21 mineralized AVs for whole-genome 5meC level using the 450 K Illumina array.[18] The data were analysed considering a region spanning the *PLPP3* gene containing 28 CpG sites. Cytosine methylation levels of two of these CpG sites were significantly associated with *PLPP3* mRNA levels, already measured using gene expression arrays (*Figure 2A*). Cytosine methylation in cg02468627, located in intron 1, was the most significant site and was inversely correlated with the expression of *PLPP3* (r = -0.51, P = 0.01) (*Figure 2B*). To confirm these findings, we measured 5meC level in cg02468627 by using bisulphite treatment and pyrosequencing in an independent series of 24 control non-mineralized and 43 mineralized AVs (*Table 2*). We found that the level of 5meC of the CpG targeted by the cg02468627 probeset was increased by 2.2-fold in CAVD (*Figure 2C*). In 28 AVs, enough tissue was available to measure both 5meC (bisulphite pyrosequencing) at the same locus (cg02468627) and *PLPP3* mRNA levels. In these AVs, the level of 5meC was inversely related with the amount of *PLPP3* mRNA (r = -0.48, P = 0.009) (*Figure 2D*). Considering that we found a lower level of *PLPP3* in the mineralized portion of CAVD, we also measured the level of 5meC of cg02468627 in macroscopically dissected pathologic AVs from non-mineralized and mineralized portions. In eight AVs, by using bisulphite pyrosequencing, we found that level of 5meC at cg02468627 was increased in the mineralized area compared with non-mineralized portion (*Figure 2E*). Hence, these data support that the level of 5meC in *PLPP3* intron 1 increases during the mineralization process of the AV and is inversely associated with its mRNA levels.

3.3 Intron 1 contains a conserved MIR transposon

Considering that cytosine methylation of intron 1 was associated with the expression of *PLPP3*, we examined the gene body sequence for TEs, which often contains regulatory motifs. The intronic cg02468627 site is located within a MIR sequence and the locus is highly conserved as shown by PhastCons analysis (*Figure 3A*). MIRs are ancient TEs, which are enriched in enhancers and within introns of genes involved in response to biotic stimulus and inflammation.[19] Histone marks were thus analysed to determine whether this intronic sequence was an enhancer. We measured in control and mineralized AVs the level of methylation (mono and tri) on lysine 4 of histone 3 (H3K4me1 and H3K4me3) by using quantitative chromatin immunoprecipitation assay (qChIP). In control and mineralized AVs, we found a high level of H3K4me1, a mark associated with enhancers, in the intron 1 region containing MIR (*Figure 3B*). Also, the level of H3K4me3, which is a mark associated with promoters and enhancers, was elevated in this region with a trend for lower levels in CAVD (P = 0.15) (*Figure 3C*). These data are consistent with a strong candidate enhancer, which is rich in both H3K4me1 and H3K4me3.[20] Crosstalk between 5meC and histone methylation has been underlined

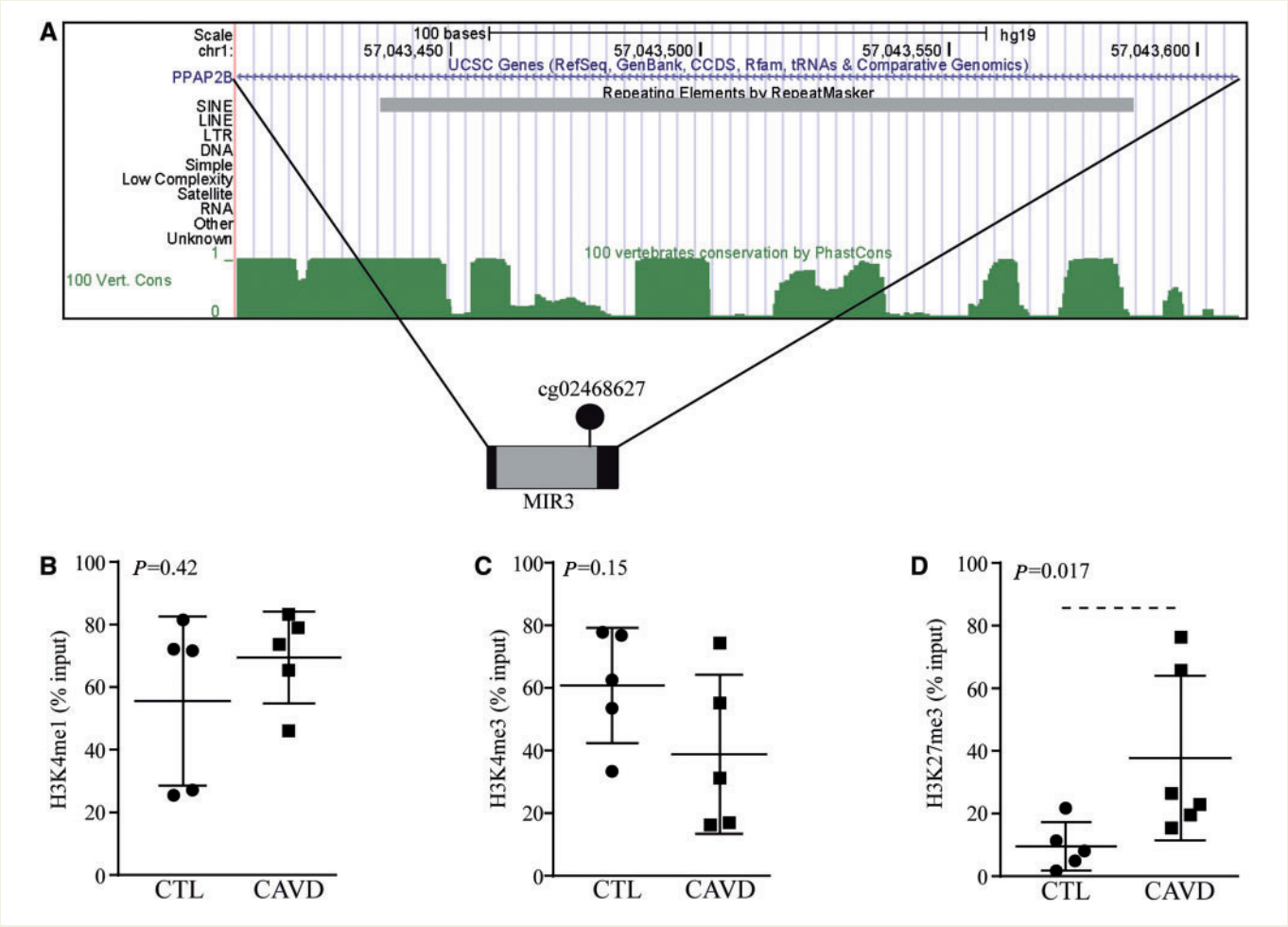

Figure 3 Intron 1 of *PLPP3* contains an enhancer. (*A*) UCSC browser image (hg19) showing cg02468627 in highly conserved region containing a MIR3 sequence. (*B–D*) H3K4me1 (CTL $n = 5$, CAVD $n = 5$) ($P = 0.42$) (*B*), H3K4me3 (CTL $n = 5$, CAVD $n = 5$) ($P = 0.15$) (*C*), and H3K27me3 (CTL $n = 5$, CAVD $n = 6$) ($P = 0.017$) (*D*) levels at MIR3 locus (determined by quantitative ChIP). Values are mean ± S.E.M., Wilcoxon-Mann-Whitney analyses; CTL, control; CAVD, calcific aortic valve disease.

and might be involved in the control of this region.[21] Polycomb repressive complex 2 (PRC2), which brings H3 trimethylation on lysine 27 (H3K27me3), is positively related to 5meC and is associated with a repressive state of chromatin.[21] By using qChIP, we documented that H3K27me3 level was weak in control AVs, whereas it was increased by 28% in the intron 1 region of CAVD (*Figure 3D*). These data are consistent with a strong enhancer in *PLPP3* intron 1 in control AVs, which is, however, repressed in mineralized AVs.

3.4 DNA methylation of intronic enhancer controls the expression of *PLPP3*

To confirm whether the intronic region is an enhancer for *PLPP3*, the intron 1 region containing MIR was cloned along with a minimal promoter from the *PLPP3* gene (-700/-140) and was coupled with the luciferase reporter gene (*Figure 4A*). The different constructions were transfected in HEK293T cells. In both forward and reverse orientations, the cloned intronic sequence increased the reporter activity by 3.6- and 3.8-fold respectively (*Figure 4A*). These data thus indicate that intron 1 contains an enhancer, which has higher 5meC level in CAVD and may regulate the expression of *PLPP3*. Next, to buttress this finding epigenome editing was performed with the clustered regularly interspersed short palindromic repeats-Cas9 system to target DNA methyltransferase (DNMT) to sequence-specific site.[22] Guide RNA (sgRNA) targeting the intron 1 enhancer was cloned in a vector containing a puromycin resistance gene and a nuclease-deficient Cas9 mutant (dCas9) fused with the active portion of DNMT3A (dCas9-DNMT) (*Figure 4B*). The control consisted in a vector containing identical target-specific sgRNA and a dCas9 fused with a catalytically inactive mutant DNMT3A (dCas9-ΔDNMT). Cells were transfected with the construction and selected with a puromycin resistance gene. When compared with the dCas9-ΔDNMT control vector, the transfection of dCas9-DNMT in HEK293T cells increased the 5meC level of cg02468627 by 13%, which was documented after 4 days by using bisulphite pyrosequencing (*Figure 4C*). The vectors encoding for dCas9-DNMT and dCas9-ΔDNMT were transfected in cells along with the enhancer reporter. When compared with the control inactive dCas9-ΔDNMT vector, the methyltransferase active vector dCas9-DNMT reduced the reporter activity by 28% (*Figure 4D*). In isolated human VICs, the transfection with dCas9-DNMT reduced *PLPP3* mRNA level by 38% (*Figure 4E*). Taken together, these data indicate that increased 5meC in intronic enhancer downregulates the expression of *PLPP3*.

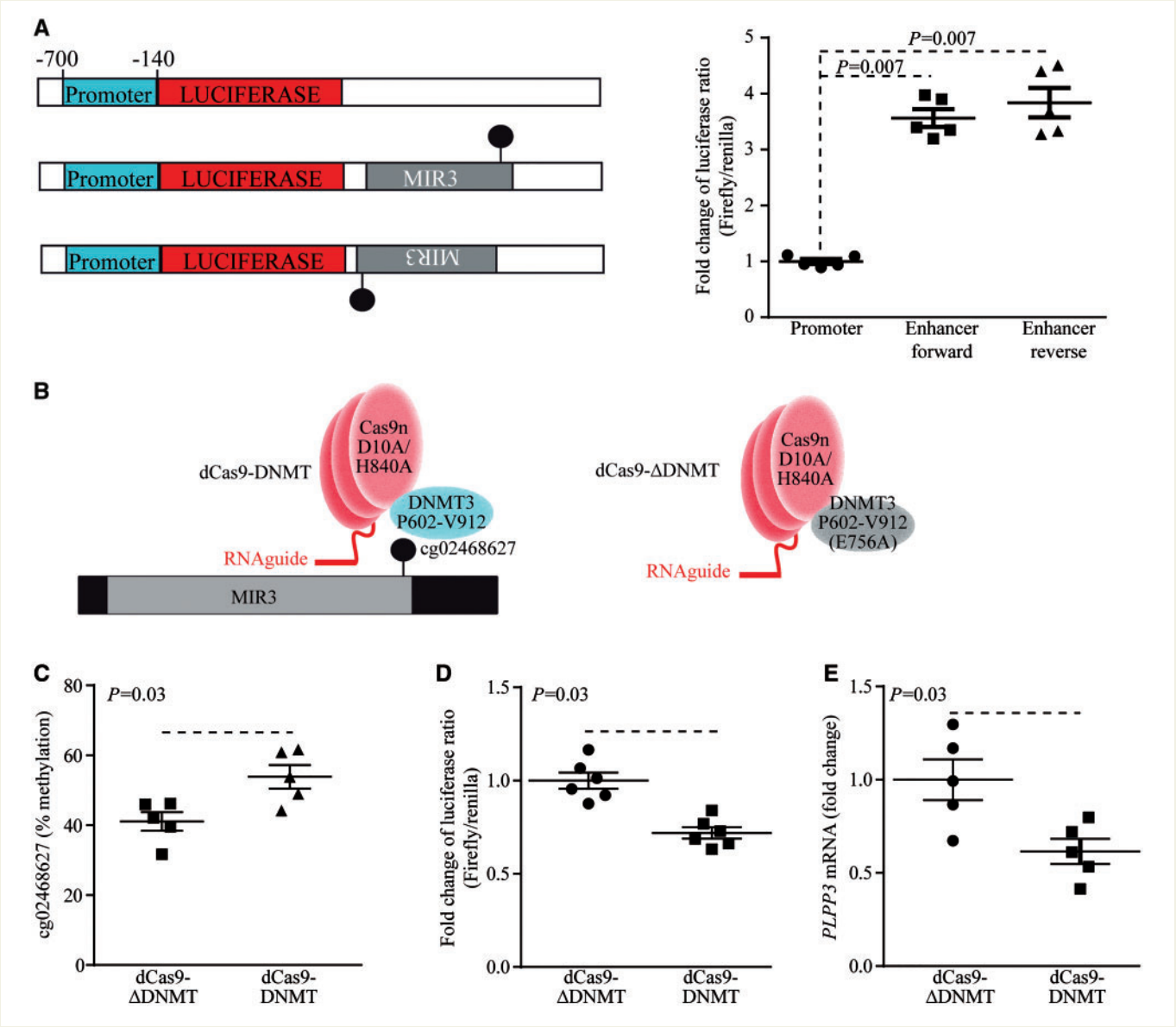

Figure 4 Intronic enhancer regulates *PLPP3* expression. (*A*) Reporter assay constructions and activities (HEK293T) ($n = 5$) ($P = 0.007$). (*B*) Scheme showing dCas9-DNMT and dCas9-ΔDNMT for epigenome editing. C) Bisulphite pyrosequencing of intronic enhancer performed in HEK293T after epigenome editing ($n = 5$) ($P = 0.03$). (*D*) Reporter assay in response to epigenome editing (HEK293T) ($n = 6$) ($P = 0.03$). (*E*) Expression of *PLPP3* in VICs in response to epigenome editing ($n = 5$) ($P = 0.03$). Values are mean ± S.E.M., Wilcoxon-Mann-Whitney analyses.

3.5 PLPP3 promotes an osteogenic programme in VICs

LysoPA is a strong promoter of osteogenic activity in VICs. We thus hypothesized that a lower PLPP3 expression level could exacerbate LysoPA-induced osteogenic activity in VICs. Human primary VICs isolated from non-mineralized AVs obtained from heart transplants were treated with LysoPA (10 μM) during 24 h and osteogenic genes were measured by RT-qPCR with and without a small interfering RNA (siRNA)-mediated knockdown of PLPP3 (*Figure 5A*). Short interfering RNA for *PLPP3* (*Figure 5A*) increased the expression of *BMP2* by 2.2-fold in response to LysoPA (*Figure 5B*). BMP2 is a strong promoter of osteogenesis and promotes the expression of *RUNX2*, a bone-related transcription factor overexpressed in human CAVD. A treatment of VICs with a siRNA targeting *PLPP3* increased LysoPA-induced expression of *RUNX2* and *BGLAP*, a downstream target of *RUNX2*, by 2.2- and 2- fold respectively (*Figure 5C* and *D*). We next evaluated the impact of PLPP3 on the mineralization process. VIC cultures were treated with a mineralizing medium containing LysoPA for 7 days and the amount of calcium deposited extracellularly was measured by the Arsenazo III method, which is specific and does not cross-react with other divalent ions, and results were normalized according to the protein levels.[18] In this assay, the knockdown of *PLPP3* increased LysoPA-induced mineralization of cell cultures by 2.8-fold (*Figure 5E*). Also, the activity of ALP, a marker of osteogenic activity, was increased by 1.9-fold in response to LysoPA after the silencing of *PLPP3* (*Figure 5F*).

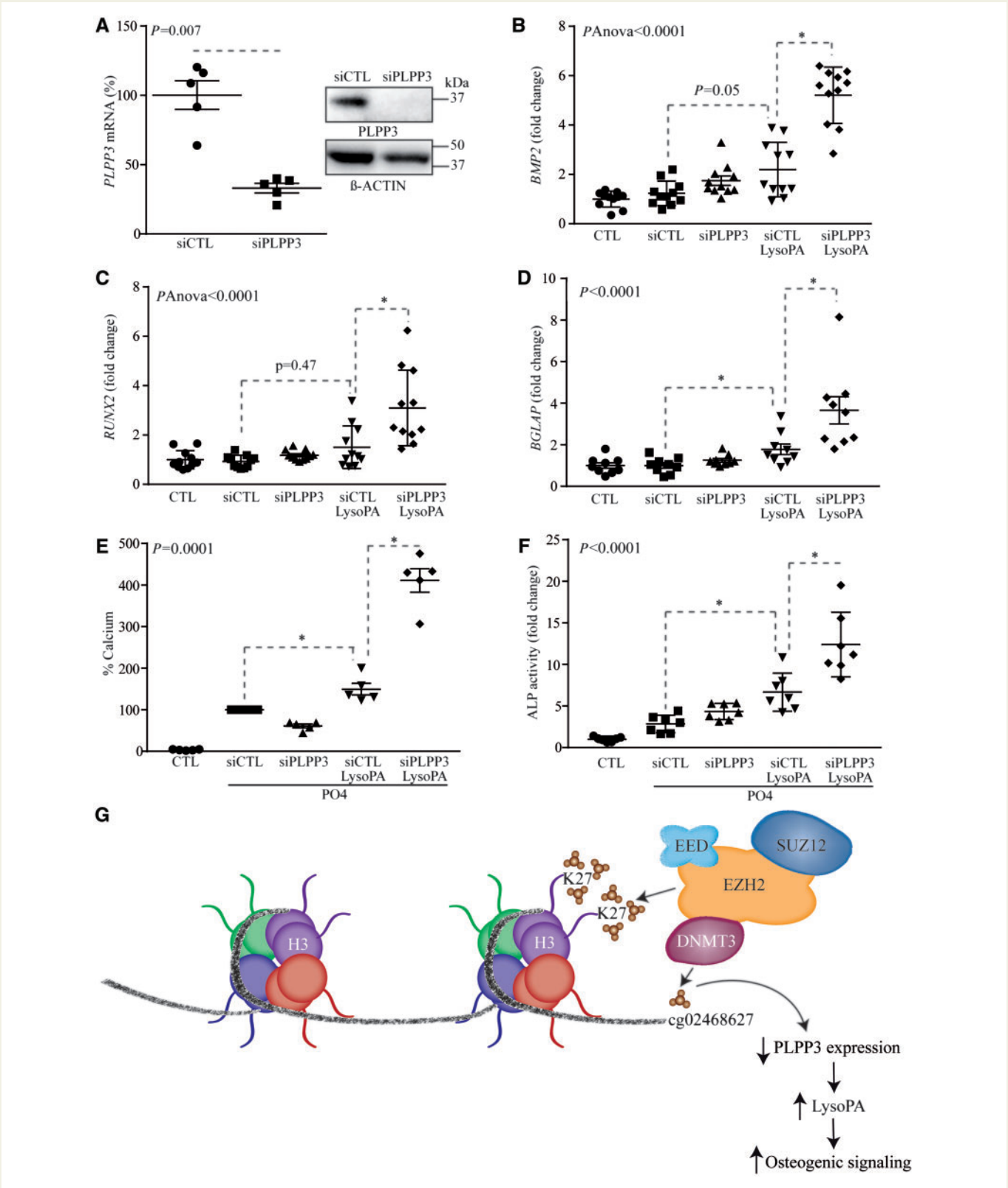

Figure 5 Lower expression of PLPP3 enhances the osteogenic transition of VICs. (*A*) siRNA-mediated knockdown on mRNA ($n = 5$) ($P = 0.007$) and protein levels. (B–D) PLPP3 siRNA on lysoPA-mediated gene expression of *BMP2* ($n = 11$) (pAnova < 0.0001) (*B*), *RUNX2* ($n = 11$) (pAnova < 0.0001) (*C*), and *BGLAP* ($n = 9$) ($P < 0.0001$) (*D*). (*E* and *F*) PLPP3 knockdown on lysoPA-induced mineralization of VIC cultures ($n = 5$) (day 7) ($P = 0.0001$) (*E*), and ALP activity ($n = 7$) (day 7) ($P < 0.0001$) (*F*). (*G*) Proposed working model showing that EZH2 (enzyme component of the PRC2 complex that increases H3K27me3) may associate with DNMT3 (*de novo* methylation of CpG) and promote silencing of *PLPP3* intronic enhancer during the mineralization of the AV. Values are mean ± S.E.M.; (*A*) Wilcoxon-Mann-Whitney analysis, (*B* and *C*) Anova, *post-hoc* Tukey, (*D–F*) Kruskal-Wallis, *post-hoc* Steel; *$P < 0.05$; LysoPA: 10 µM; PO4 is mineralizing medium (PO4 2 mM); percentage of calcium in (*E*) is indicated and represents a surrogate of mineralization (hydroxyapatite of calcium) that is deposited by VICs.

4. Discussion

In this work, we highlighted a novel process whereby the osteogenic transition of VICs is promoted by a downregulation of PLPP3. We found that a CpG site located in an intronic MIR-based enhancer is methylated and has a repressive chromatin state consisting in H3K27me3 in CAVD. Cytosine methylation of intronic enhancer actively participates to the downregulation of *PLPP3* during the mineralization of the AV. Epigenome editing of MIR-based enhancer by using dCas9-DNMT reduced the expression of *PLPP3* in VICs. In turn, reduced expression of *PLPP3* in human VICs promoted the expression of osteogenic genes and the mineralization of cell cultures. Taken together, these data support that epigenetic silencing of an intronic enhancer in *PLPP3* promotes an osteogenic programme in the AV (*Figure 5G*).

4.1 Acquired dysregulation of *PLPP3* expression during mineralization of the AV

Comprehensive analyses in human AVs showed that in addition to mRNA, PLPP3 protein level, and enzymatic activity were also downregulated in pathologic specimen. In order to decipher the process whereby PLPP3 was dysregulated in CAVD we generated a multidimensional dataset including gene expression and genome-wide DNA methylation array. This analysis showed that 5meC level in cg02468627, located in intron 1 of *PLPP3*, was associated with gene expression level in CAVD. By using bisulphite pyrosequencing in a different set of 24 control and 43 mineralized AVs we confirmed that 5meC level at cg02468627 was increased by 2.2-fold in CAVD and was inversely associated with the expression of *PLPP3*. Of interest, analyses performed among pathologic leaflets showed that the mineralized portion had reduced expression of *PLPP3*. Incidentally, 5meC was also increased in mineralized portion compared with non-mineralized area of pathologic AVs. These data thus underscored that during the mineralization process of the AV, cytosine methylation in intron 1 is increased and this concomitantly with a reduction in *PLPP3* expression.

4.2 Intron 1 contains a MIR-based enhancer for *PLPP3*

TEs, which comprise >45% of the genome, have been exapted for different control functions.[5] To this effect, TEs of the MIR family are enriched in enhancers.[6] Enhancers, which are located in large intergenic regions or within the introns, exert crucial regulatory role on the expression of genes. Previous work has shown that rs72664324, a gene variant located in intron 5 of *PLPP3* and in high linkage disequilibrium with rs17114036, a single nucleotide polymorphism with a genome-wide significant association with coronary artery disease, is located in an enhancer that regulates the expression of *PLPP3*.[23] In this work, we discovered a novel enhancer located in intron 1 of *PLPP3*, which is epigenetically silenced during CAVD. In reporter assay, MIR located in intron 1 increased the activity of a minimal promoter by 3.6-fold in an orientation-independent manner, which is consistent with an enhancer. In AVs, this locus has high levels of H3K4me1 and H3K4me3, which are epigenetic marks of strong enhancer.[20]

4.3 5meC and H3K27me3 at intronic enhancer in CAVD

Analyses of intronic enhancer at *PLPP3* showed that a high level of 5meC was accompanied by an increased H3K27me3 level in CAVD. H3K27me3 is a repressive mark deposited by PRC2 often in the context of increased 5meC.[21] We have used epigenome editing with dCas9-DNMT to probe the role of 5meC at intronic MIR-based enhancer.[22] Of interest, dCas9-DNMT increased 5meC at cg02468627 by 13% and decreased enhancer reporter activity by 41%. In VICs, dCas9-DNMT reduced significantly the expression of *PLPP3*. Taken together, these data strongly suggest that increased methylation of a MIR-based enhancer in intron 1 exerts a control on the expression of *PLPP3*. Whether or not trimethylation on lysine 27 of histone 3 (H3K27me3) at the same locus is necessary or exacerbate the knockdown of *PLPP3* is, however, unknown and warrants further investigation.

4.4 PLPP3 is a regulator of osteogenic transition

Studies have shown that Lp(a), which transports a large fraction of OxPLs in the bloodstream, is causally associated with CAVD.[10] Investigations have underscored that ATX binds to Lp(a) and promotes the production of LysoPA in the AVs.[13] LysoPA produced by ATX is a strong promoter of osteogenic transition in VICs. We recently identified that LysoPA derived from the OxLDL promotes in VICs the expression of BMP2, a potent morphogen that drives an osteogenic programme.[15] In this work, we hypothesized that LysoPA signalling in the AV could be modulated by the expression of PLPPs. We found that PLPP3 was downregulated in VICs during CAVD and exacerbated the osteogenic transition of cells in response to LysoPA. In this regard, a knockdown of *PLPP3* with siRNA increased LysoPA-induced expression of key drivers of mineralization such as *BMP2* and *RUNX2*. Consistently, LysoPA-induced mineralization of VIC culture was exacerbated by the knockdown of *PLPP3*. Hence, these data indicates that PLPP3 is a key modulator of osteogenic fate in VICs.

4.5 Limitations

In this work, we delineated the role of a key regulator of LysoPA signalling. These data were obtained by using comprehensive analyses of human AVs and *in vitro* experiments conducted with human primary VICs. Whether the expression of PLPP3 could be modulated and whether it could impact on the development of CAVD *in vivo* is actually unknown. However, recent works in a preclinical mouse model of CAVD showed that circulating level of LysoPA is increased and the blockade of this pathway prevented the progression of AV mineralization.[15] Also, it is worth highlighting that some variables, difficult to control for, may have affected the results. For instance, DNA methylation in tissues could differ according to cell types[24] and following the plating of VICs, a heterogeneous cell population, the epigenetic memory could change.[7] Hence, further work is needed to elucidate the processes whereby *PLPP3* is epigenetically silenced in CAVD. In the end, it may help design novel therapies that would modulate LysoPA signalling.

5. Conclusion

The expression of *PLPP3* is decreased in CAVD and promotes the osteogenic transition of VICs. We discovered a novel intronic enhancer, which has increased 5meC level in CAVD and exerts an important control over the expression of *PLPP3*. Gene reprogramming of VICs at *PLPP3* enhancer may hold promise for the development of novel epigenetic-based therapies.

Supplementary material

Supplementary material is available at Cardiovascular Research online.

Authors' contributions

G.M., M.C.B., and P.M. conceived and designed experiments. G.M. performed cell culture experiments and qChIP. G.M. and M.C.B. performed genome editing experiments. G.M. performed luciferase reporter assays. V.G.O. and L.B. performed pysosequencing experiments. M.J.N. performed mineralization experiments. G.M., F.H., D.A., and G.R. performed qPCRs. N.G. and Y.B. generated multidimensional datasets including transcriptomic and 5meC array. G.M. and M.R. generated tables. M.C.B. generated the figures. P.M. drafted the article. All the authors critically reviewed the article and provided scientific input.

Acknowledgements

This work was supported by CIHR grants to P.M. (MOP114893, MOP245048, MOP341860, and MOP365029) the Heart and Stroke Foundation of Canada and the Quebec Heart and Lung Institute Fund. LB is a junior research scholar from the Fonds de la recherche du Québec en santé (FRQS) and a member of the FRQS-funded Centre de recherche du CHUS (affiliated to the Centre hospitalier universitaire de Sherbrooke). VGO received a doctoral research award from FRQS. Y.B. holds a Canada Research Chair in Genomics of Heart and Lung Diseases. P.M. holds a FRQS Research Chair on the Pathobiology of Calcific Aortic Valve Disease.

Conflict of interest: none declared.

References

1. Mathieu P, Boulanger MC. Basic mechanisms of calcific aortic valve disease. *Can J Cardiol* 2014;**30**:982–993.
2. Migicovsky Z, Kovalchuk I. Epigenetic memory in mammals. *Front Genet* 2011;**2**:28.
3. Nagy E, Back M. Epigenetic regulation of 5-lipoxygenase in the phenotypic plasticity of valvular interstitial cells associated with aortic valve stenosis. *FEBS Lett* 2012;**586**:1325–1329.
4. Hon GC, Rajagopal N, Shen Y, McCleary DF, Yue F, Dang MD, Ren B. Epigenetic memory at embryonic enhancers identified in DNA methylation maps from adult mouse tissues. *Nat Genet* 2013;**45**:1198–1206.
5. Feschotte C. Transposable elements and the evolution of regulatory networks. *Nat Rev Genet* 2008;**9**:397–405.
6. Jjingo D, Conley AB, Wang J, Marino-Ramirez L, Lunyak VV, Jordan IK. Mammalian-wide interspersed repeat (MIR)-derived enhancers and the regulation of human gene expression. *Mob DNA* 2014;**5**:14.
7. Lee HJ, Hore TA, Reik W. Reprogramming the methylome: erasing memory and creating diversity. *Cell Stem Cell* 2014;**14**:710–719.
8. Bosse Y, Miqdad A, Fournier D, Pepin A, Pibarot P, Mathieu P. Refining molecular pathways leading to calcific aortic valve stenosis by studying gene expression profile of normal and calcified stenotic human aortic valves. *Circ Cardiovasc Genet* 2009;**2**:489–498.
9. Guauque-Olarte S, Droit A, Tremblay-Marchand J, Gaudreault N, Kalavrouziotis D, Dagenais F, Seidman JG, Body SC, Pibarot P, Mathieu P, Bossé Y. RNA expression profile of calcified bicuspid, tricuspid, and normal human aortic valves by RNA sequencing. *Physiol Genomics* 2016;**48**:749–761.
10. Thanassoulis G, Campbell CY, Owens DS, Smith JG, Smith AV, Peloso GM, Kerr KF, Pechlivanis S, Budoff MJ, Harris TB, Malhotra R, O'Brien KD, Kamstrup PR, Nordestgaard BG, Tybjaerg-Hansen A, Allison MA, Aspelund T, Criqui MH, Heckbert SR, Hwang SJ, Liu Y, Sjogren M, van der Pals J, Kalsch H, Muhleisen TW, Nothen MM, Cupples LA, Caslake M, Di AE, Danesh J, Rotter JI, Sigurdsson S, Wong Q, Erbel R, Kathiresan S, Melander O, Gudnason V, O'Donnell CJ, Post WS. Genetic associations with valvular calcification and aortic stenosis. *N Engl J Med* 2013;**368**:503–512.
11. Smith JG, Luk K, Schulz C-A, Engert JC, Do R, Hindy G, Rukh G, Dufresne L, Almgren P, Owens DS, Harris TB, Peloso GM, Kerr KF, Wong Q, Smith AV, Budoff MJ, Rotter JI, Cupples LA, Rich S, Kathiresan S, Orho-Melander M, Gudnason V, O'donnell CJ, Post WS, Thanassoulis G. Association of low-density lipoprotein cholesterol-related genetic variants with aortic valve calcium and incident aortic stenosis. *Jama* 2014;**312**:1764–1771.
12. Mathieu P, Arsenault BJ, Boulanger MC, Bosse Y, Koschinsky ML. Pathobiology of Lp(a) in calcific aortic valve disease. *Expert Rev Cardiovasc Ther* 2017;**15**:797–807.
13. Bouchareb R, Mahmut A, Nsaibia MJ, Boulanger MC, Dahou A, Lepine JL, Laflamme MH, Hadji F, Couture C, Trahan S, Page S, Bosse Y, Pibarot P, Scipione CA, Romagnuolo R, Koschinsky ML, Arsenault BJ, Marette A, Mathieu P. Autotaxin derived from lipoprotein(a) and valve interstitial cells promotes inflammation and mineralization of the aortic valve. *Circulation* 2015;**132**:677–690.
14. Nsaibia MJ, Mahmut A, Boulanger MC, Arsenault BJ, Bouchareb R, Simard S, Witztum JL, Clavel MA, Pibarot P, Bosse Y, Tsimikas S, Mathieu P. Autotaxin interacts with lipoprotein(a) and oxidized phospholipids in predicting the risk of calcific aortic valve stenosis in patients with coronary artery disease. *J Intern Med* 2016;**280**:509–517.
15. Nsaibia MJ, Boulanger MC, Bouchareb R, Mkannez G, Le QK, Hadji F, Argaud D, Dahou A, Bosse Y, Koschinsky ML, Pibarot P, Arsenault BJ, Marette A, Mathieu P. OxLDL-derived lysophosphatidic acid promotes the progression of aortic valve stenosis through a LPAR1-RhoA-NF-kappaB pathway. *Cardiovasc Res* 2017;**113**:1351–1363.
16. Brindley DN, Pilquil C. Lipid phosphate phosphatases and signaling. *J Lipid Res* 2009;**50** Suppl:S225–S230.
17. Guauque-Olarte S, Messika-Zeitoun D, Droit A, Lamontagne M, Tremblay-Marchand J, Lavoie-Charland E, Gaudreault N, Arsenault BJ, Dubé M-P, Tardif J-C, Body SC, Seidman JG, Boileau C, Mathieu P, Pibarot P, Bossé Y. Calcium signaling pathway genes RUNX2 and CACNA1C are associated with calcific aortic valve disease. *Circ Cardiovasc Genet* 2015;**8**:812–822.
18. Hadji F, Boulanger M-C, Guay S-P, Gaudreault N, Amellah S, Mkannez G, Bouchareb R, Marchand JT, Nsaibia MJ, Guauque-Olarte S, Pibarot P, Bouchard L, Bossé Y, Mathieu P. Altered DNA methylation of long noncoding RNA H19 in calcific aortic valve disease promotes mineralization by silencing NOTCH1. *Circulation* 2016;**134**:1848–1862.
19. Sironi M, Menozzi G, Comi GP, Cereda M, Cagliani R, Bresolin N, Pozzoli U. Gene function and expression level influence the insertion/fixation dynamics of distinct transposon families in mammalian introns. *Genome Biol* 2006;**7**:R120.
20. Ernst J, Kheradpour P, Mikkelsen TS, Shoresh N, Ward LD, Epstein CB, Zhang X, Wang L, Issner R, Coyne M, Ku M, Durham T, Kellis M, Bernstein BE. Mapping and analysis of chromatin state dynamics in nine human cell types. *Nature* 2011;**473**:43–49.
21. Vire E, Brenner C, Deplus R, Blanchon L, Fraga M, Didelot C, Morey L, Van EA, Bernard D, Vanderwinden JM, Bollen M, Esteller M, Di CL, de LY, Fuks F. The Polycomb group protein EZH2 directly controls DNA methylation. *Nature* 2006;**439**:871–874.
22. Vojta A, Dobrinic P, Tadic V, Bockor L, Korac P, Julg B, Klasic M, Zoldos V. Repurposing the CRISPR-Cas9 system for targeted DNA methylation. *Nucleic Acids Res* 2016;**44**:5615–5628.
23. Reschen ME, Gaulton KJ, Lin D, Soilleux EJ, Morris AJ, Smyth SS, O'Callaghan CA. Lipid-induced epigenomic changes in human macrophages identify a coronary artery disease-associated variant that regulates PPAP2B Expression through Altered C/EBP-beta binding. *PLoS Genet* 2015;**11**:e1005061.
24. Pan S, Lai H, Shen Y, Breeze C, Beck S, Hong T, Wang C, Teschendorff AE. DNA methylome analysis reveals distinct epigenetic patterns of ascending aortic dissection and bicuspid aortic valve. *Cardiovasc Res* 2017;**113**:692–704.